Video Article

# Pretargeted Radioimmunotherapy Based on the Inverse Electron Demand Diels-Alder Reaction

Rosemery Membreno[1,2], Brendon E. Cook[1,2,3], Brian M. Zeglis[1,2,3,4]

[1]Department of Chemistry, Hunter College of the City University of New York

[2]Ph.D. Program in Chemistry, Graduate Center of the City University of New York

[3]Department of Radiology, Memorial Sloan Kettering Cancer Center

[4]Department of Radiology, Weill Cornell Medical College

Correspondence to: Brian M. Zeglis at bz102@hunter.cuny.edu

URL: https://www.jove.com/video/59041
DOI: doi:10.3791/59041

Keywords: radioimmunotherapy, pretargeted radioimmunotherapy, pretargeting, inverse electron demand Diels-Alder reaction, tetrazine, *trans*-cyclooctene, huA33, A33 antigen, lutetium-177

Date Published: 10/22/2018

Citation: Membreno, R., Cook, B.E., Zeglis, B.M. Pretargeted Radioimmunotherapy Based on the Inverse Electron Demand Diels-Alder Reaction. *J. Vis. Exp.* (), e59041, doi:10.3791/59041 (2018).

## Abstract

While radioimmunotherapy (RIT) is a promising approach for the treatment of cancer, the long pharmacokinetic half-life of radiolabeled antibodies can result in high radiation doses to healthy tissues. Perhaps not surprisingly, several different strategies have been developed to circumvent this troubling limitation. One of the most promising of these approaches is pretargeted radioimmunotherapy (PRIT). PRIT is predicated on decoupling the radionuclide from the immunoglobulin, injecting them separately, and then allowing them to combine *in vivo* at the target tissue. This approach harnesses the exceptional tumor-targeting properties of antibodies while skirting their pharmacokinetic drawbacks, thereby lowering radiation doses to non-target tissues and facilitating the use of radionuclides with half-lives that are considered too short for use in traditional radioimmunoconjugates. Over the last five years, our laboratory and others have developed an approach to *in vivo* pretargeting based on the inverse electron-demand Diels-Alder (IEDDA) reaction between *trans*-cyclooctene (TCO) and tetrazine (Tz). This strategy has been successfully applied to pretargeted positron emission tomography (PET) and single-photon emission computed tomography (SPECT) imaging with a variety of antibody-antigen systems. In a pair of recent publications, we have demonstrated the efficacy of IEDDA-based PRIT in murine models of pancreatic ductal adenocarcinoma and colorectal carcinoma. In this protocol, we describe protocols for PRIT using a $^{177}$Lu-DOTA-labeled tetrazine radioligand ([$^{177}$Lu]Lu-DOTA-PEG$_7$-Tz) and a TCO-modified variant of the colorectal cancer targeting huA33 antibody (huA33-TCO). More specifically, we will describe the construction of huA33-TCO, the synthesis and radiolabeling of [$^{177}$Lu]Lu-DOTA-PEG$_7$-Tz, and the performance of *in vivo* biodistribution and longitudinal therapy studies in murine models of colorectal carcinoma.

## Introduction

Radioimmunotherapy (RIT) — the use of antibodies for the delivery of therapeutic radionuclides to tumors — has long been an enticing approach to the treatment of cancer[1,2]. Indeed, this promise has been underscored by the United States Food and Drug Administration's approval of two radioimmunoconjugates for the treatment of Non-Hodgkin's Lymphoma: $^{90}$Y-ibritumomab tiuxetan and $^{131}$I-tositumomab[3,4]. Yet even from its earliest days, the clinical prospects of RIT have been hampered by a critical complication: high radiation dose rates to healthy tissues[5,6]. Generally speaking, radioimmunoconjugates for RIT are labeled with long-lived radionuclides (*e.g.*, $^{131}$I [$t_{½}$ = 8.0 days] and $^{90}$Y [$t_{½}$ = 2.7 days]) with physical half-lives that dovetail well with the long pharmacokinetic half-lives of immunoglobulins. This is essential, as it ensures that sufficient radioactivity remains once the antibody has reached its optimal biodistribution after several days of circulation. However, this combination of long residence times in the blood and long physical half-lives inevitably results in the irradiation of healthy tissues, thereby reducing therapeutic ratios and limiting the efficacy of therapy[7]. Several strategies have been explored to circumvent this problem, including the use of truncated antibody fragments such as Fab, Fab', F(ab')$_2$, minibodies, and nanobodies[8,9,10]. One of the most promising and fascinating, yet undeniably complex, alternative approaches is *in vivo* pretargeting[11].

*In vivo* pretargeting is an approach to nuclear imaging and therapy that seeks to harness the exquisite affinity and selectivity of antibodies while skirting their pharmacokinetic drawbacks[11,12,13]. To this end, the radiolabeled antibody used in traditional radioimmunotherapy is deconstructed into two components: a small molecule radioligand and an immunoconjugate that can bind *both* a tumor antigen and the aforementioned radioligand. The immunoconjugate is injected first and given a 'head start', often several days, during which it accumulates in the target tissue and clears from the blood. Subsequently, the small molecule radioligand is administered and either combines with the immunoconjugate at the tumor or rapidly clears from the body. In essence, *in vivo* pretargeting relies upon performing radiochemistry within the body itself. By reducing the circulation of the radioactivity, this approach simultaneously reduces radiation doses to healthy tissues and facilitates the use of radionuclides (*e.g.*, $^{68}$Ga, $t_{½}$ = 68 min[211]; As, $t_{½}$ = 7.2 h) with half-lives that are typically considered incompatible with antibody-based vectors.

Starting in the late 1980s, a handful of different approaches to *in vivo* pretargeting have been developed, including strategies based on bispecific antibodies, the interaction between streptavidin and biotin, and the hybridization of complementary oligonucleotides[14,15,16,17,18]. Yet each has been held back to varying degrees by complications, most famously the potent immunogenicity of streptavidin-modified antibodies[19,20]. Over the last five years, our group and others have developed an approach to *in vivo* pretargeting based on the rapid and bioorthogonal inverse

 

electron demand Diels-Alder ligation between *trans*-cyclooctene (TCO) and tetrazine (Tz)[21,22,23,24]. The most successful of these strategies have employed a TCO-modified antibody and a Tz-bearing radioligand, as TCO is typically more stable *in vivo* than its Tz partner (**Figure 1**)[25,26]. As in other pretargeting methodologies, the mAb-TCO immunoconjugate is administered first and given time to clear from circulation and accumulate in tumor tissue. Subsequently, the small molecule Tz radioligand is injected, after which it either clicks with the immunoconjugate within the target tissue or clears rapidly from the body. This *in vivo* pretargeting strategy has proven highly effective for PET and SPECT imaging with several different antibody/antigen systems, consistently producing images with high contrast and enabling the use of short-lived radionuclides such as $^{18}$F ($t_{½}$ = 109 min) and $^{64}$Cu ($t_{1/2}$ = 12.7 h)[21,22,24]. More recently, the efficacy of click-based pretargeted radioimmunotherapy (PRIT) has been demonstrated in murine models of pancreatic ductal adenocarcinoma (PDAC) and colorectal carcinoma[27,28]. To this end, the therapeutic radionuclide $^{177}$Lu ($b_{max}$ = 498 keV, $t_{1/2}$ = 6.7 days) was employed in conjunction with two different antibodies: 5B1, which targets carbohydrate antigen 19.9 (CA19.9) ubiquitously expressed in PDAC, and huA33, which targets A33, a transmembrane glycoprotein expressed in >95% of colorectal cancers. In both cases, this approach to $^{177}$Lu-PRIT yielded high activity concentrations in tumor tissue, created a dose-dependent therapeutic effect, and simultaneously reduced activity concentrations in healthy tissues compared to traditional directly-labeled radioimmunoconjugates.

In this article, we describe protocols for PRIT using a $^{177}$Lu-DOTA-labeled tetrazine radioligand ([$^{177}$Lu]Lu-DOTA-PEG$_7$-Tz) and a TCO-modified variant of the huA33 antibody (huA33-TCO). More specifically, we describe the construction of huA33-TCO (**Figure 2**), the synthesis and radiolabeling of [$^{177}$Lu]Lu-DOTA-PEG$_7$-Tz (**Figure 3** and **Figure 4**), and the performance of *in vivo* biodistribution and longitudinal therapy studies in murine models of colorectal carcinoma. Furthermore, in the representative results and discussion, we present a sample data set, address possible strategies for the optimization of this approach, and consider this strategy in the wider context of *in vivo* pretargeting and PRIT. Finally, it is important to note that while we have chosen to focus on pretargeting using huA33-TCO and [$^{177}$Lu]Lu-DOTA-PEG$_7$-Tz in this protocol, this strategy is highly modular and can be adapted to suit a wide range of antibodies and radionuclides.

## Protocol

All *in vivo* animal experiments described in this work were performed according to approved protocols and executed under the ethical guidelines of the Memorial Sloan Kettering Cancer Center, Weill Cornell Medical Center, and Hunter College Institutional Animal Care and Use Committees (IACUC).

# 1. The preparation of huA33-TCO

NOTE: The synthesis of huA33-TCO has been previously reported[29]. However, for the ease of the reader, it is replicated here with adjustments for optimal conditions.

1. In a 1.7 mL microcentrifuge tube, prepare a 125 µL solution of (*E*)-cyclooct-4-enyl 2,5-dioxo-1-pyrrolidinyl carbonate (TCO-NHS) in dry dimethyl formamide (DMF) at a concentration of 40 mg/mL (0.15 M). This solution can be aliquoted and frozen at -80 °C for use in future experiments.
2. In a separate 1.7 mL microcentrifuge tube, prepare a 5 mg/mL solution of huA33 in 1 mL of phosphate buffered saline (PBS; 2.7 mM potassium chloride, 137 mM sodium chloride, and 11.9 mM potassium phosphate, pH 7.4).
3. Using small aliquots (<5 µL) of 0.1 M $Na_2CO_3$, adjust the pH of the antibody solution from Step 1.2 to 8.8-9.0. Use either pH paper or a pH meter with a microelectrode to monitor the pH and exercise care that the pH does not exceed 9.0.
4. To the antibody solution described in Step 1.3, slowly add a volume corresponding to 40 molar equivalents of TCO-NHS relative to the amount of antibody. For example, if 5 mg (30 nmol) of huA33 is in the solution, add 9.0 µL (1.20 µmol) of the 40 mg/mL (0.15 M) solution of TCO-NHS.
   NOTE: TCO-NHS is hydrophobic. When adding it to the solution of antibody, add it slowly and with agitation to prevent precipitation. Do not exceed 10% DMF by volume in the final reaction solution.
5. Allow the reaction to incubate at 25 °C on a thermomixer for 1 h with mild agitation (500 rpm).
6. After 1 h, purify the huA33-TCO immunoconjugate using a pre-packed disposable size exclusion desalting column.
   1. Equilibrate the size exclusion column as described by the supplier to remove any preservatives present in the column during storage. A typical procedure involves washing the column 5x with a volume of PBS that corresponds to the volume of the column: 5 x 2.5 mL of PBS.
   2. Add the reaction mixture to the size exclusion column noting the volume of the reaction mixture.
   3. After the reaction mixture has entered the column, add an appropriate amount of PBS to bring the total volume of solution added to the column up to 2.5 mL. For example, if the conjugation reaction resulted in a total volume of 1.3 mL, add 1.2 mL of additional PBS to the column.
   4. Collect the product using 2 mL of PBS as the eluent.
      NOTE: This step will yield the final construct huA33-TCO in 2 mL of PBS, pH 7.4.
7. Measure the concentration of the huA33-TCO using a UV-Vis spectrophotometer monitoring the 280 nm wavelength. The molar extinction coefficient for most IgGs ($e_{280}$) is 210,000 $M^{-1}cm^{-1}$.
8. If a solution with a higher concentration of immunoconjugate is desired, concentrate the huA33-TCO solution using a centrifugal filter unit with a 50,000 molecular weight cut-off following manufacturer instructions.
   NOTE: Many antibodies have been known to aggregate or precipitate during concentration. When attempting this procedure with a new antibody, researchers should defer to the literature or their own experience handling the antibody in question.
9. Store the completed huA33-TCO immunoconjugate at 4 °C in the dark if it is needed immediately. If it is to be used more than 4 days in the future, store it at -80 °C in the dark.
   NOTE: This is an acceptable stopping point in the procedure. The completed huA33-TCO immunoconjugate should be stable for at least 6 months storage at -80 °C in the dark.

## 2. The Synthesis of Tz-PEG$_7$-NHBoc

1. In a 1.7 mL microcentrifuge tube, dissolve 5 mg of tetrazine *N*-hydroxysuccinimidyl ester (Tz-NHS; 12.6 µmol) in 0.15 mL of anhydrous dimethyl sulfoxide (DMSO).
2. In a separate 1.7 mL microcentrifuge tube, dissolve 8 mg of Boc-protected amino PEG polymer (Boc-NH-PEG$_7$-NH$_2$; 17.1 µmol) in 0.15 mL of anhydrous DMSO.
3. To the solution of Tz-NHS, add 3 µL (21.3 µmol, 1.7 molar equivalents) of triethylamine (TEA) and mix thoroughly.
4. Add the pink tetrazine solution to the NHBoc-PEG$_7$-NH$_2$ solution from Step 2.2 and incubate the reaction mixture for 30 min at room temperature (RT) with mild agitation.
5. After 30 minutes, dilute the reaction 1:1 in $H_2O$ and purify the reaction using reversed-phase $C_{18}$ high-performance liquid chromatography (HPLC) to separate any unreacted Tz-NHS from the Tz-PEG$_7$-NHBoc. Use solvents without acid to prevent the premature removal of the Boc protecting group. Monitor both Tz-PEG$_7$-NHBoc and Tz-NHS at a wavelength of 525 nm.
   NOTE: Retention times are obviously highly dependent on the HPLC equipment of each laboratory (pumps, columns, tubing, *etc*.), and appropriate controls should be run prior to purification. However, to present an example, if a gradient of 5:95 MeCN/$H_2O$ (both **without** any additive) to 95:5 MeCN/$H_2O$ over 30 min, a flow rate of 1 mL/min, and an analytical 4.6 mm x 250 mm $C_{18}$column are used, the retention times of Tz-NHS and Tz-PEG$_7$-NHBoc are around 16 min and 18 min, respectively.
6. Freeze the collected HPLC eluent using liquid nitrogen and wrap the now-frozen collection tube in aluminum foil. Place the frozen collection tube on a lyophilizer overnight to remove the HPLC mobile phase. The product will be a characteristic bright pink solid.
   NOTE: If liquid nitrogen is not available, freeze the collected HPLC eluent in dry ice or overnight in a -80 °C freezer.

## 3. The Synthesis of Tz-PEG$_7$-NH$_2$

1. To the product from Step 2.6, Tz-PEG$_7$-NHBoc, add 1.5 mL of dichloromethane (DCM) and transfer this solution to a small round-bottom flask.
2. Add 0.25 mL of trifluoroacetic acid (TFA) dropwise to the pink solution from Step 3.1.
3. Allow the reaction to incubate for 30 min at RT with mild agitation.
4. After 30 min, evaporate the solvent *via* rotary evaporation. Do not exceed a water bath temperature of 37 °C.
5. Reconstitute the pink viscous product in 0.5 mL of water.
6. Purify the product using reversed-phase $C_{18}$ HPLC to separate Tz-PEG$_7$-NH$_2$ from the Boc-protected precursor. Monitor both Tz-PEG$_7$-NHBoc and Tz-PEG$_7$-NH$_2$ at a wavelength of 525 nm.
   NOTE: Retention times are obviously highly dependent on the HPLC equipment of each laboratory (pumps, columns, tubing, *etc*.), and appropriate controls should be run prior to purification. However, to present an example, if a gradient of 5:95 MeCN/$H_2O$ (both **without** any additive) to 95:5 MeCN/$H_2O$ over 30 min, a flow rate of 1 mL/min, and an analytical 4.6 mm x 250 mm $C_{18}$column are used, the retention times of Tz-PEG$_7$-NHBoc and Tz-PEG$_7$-NH$_2$ are around 18 min and 13 min, respectively.
7. Freeze the collected HPLC eluent using liquid nitrogen and wrap the now-frozen collection tube in aluminum foil. Place the frozen collection tube on a lyophilizer overnight to remove the HPLC mobile phase. The product will be a bright pink solid.
8. Reconstitute the product from Step 3.7, Tz-PEG$_7$-NH$_2$, with 150 µL of DMSO and transfer to a 1.7 mL microcentrifuge tube.
9. Measure the concentration of Tz-PEG$_7$-NH$_2$ using a UV-Vis spectrophotometer monitoring the 525 nm wavelength. The molar extinction coefficient for Tz-PEG$_7$-NH$_2$ ($e_{525}$) is 535 $M^{-1}cm^{-1}$.

## 4. The Synthesis of Tz-PEG$_7$-DOTA

1. Dissolve Tz-PEG$_7$-NH$_2$ (4.5 mg, 6.9 µmol) in 0.15 mL of DMSO (or simply proceed with the solution created in Step 3.8).
2. Add 22 molar equivalents of TEA (21 µL, 0.15 mmol) to the tetrazine-containing solution from Step 4.1.
3. Add 10 mg (14.2 µmol) of *p*-SCN-Bn-DOTA as a solid and vortex the solution for about 2 min or until the material is fully dissolved.
4. Allow the reaction to incubate for 30 min at RT with mild agitation.
5. After 30 min, dilute the reaction 1:1 in $H_2O$ and purify the product using reversed-phase $C_{18}$ HPLC to remove unreacted *p*-SCN-Bn-DOTA. The *p*-SCN-Bn-DOTA can be monitored at a wavelength of 254 nm, while the Tz-PEG$_7$-DOTA is best monitored at a wavelength of 525 nm.
   NOTE: Retention times are obviously highly dependent on the HPLC equipment of each laboratory (pumps, columns, tubing, *etc*.), and appropriate controls should be run prior to purification. However, to present an example, if a gradient of 5:95 MeCN/$H_2O$ (both **without** any additive) to 95:5 MeCN/$H_2O$ over 30 min and an analytical 4.6 x 250 mm $C_{18}$column are used, Tz-PEG$_7$-DOTA and p-SCN-Bn-DOTA have retention times of around 15.6 min and 16.1 min, respectively.
6. Freeze the collected HPLC eluent using liquid nitrogen and wrap the now-frozen collection tube in aluminum foil. Place the frozen collection tube on a lyophilizer overnight to remove the HPLC mobile phase. The product will be a bright pink powder.
7. Reconstitute the product in 0.15 mL of DMSO and measure the concentration using a UV-Vis spectrophotometer monitoring the 525 nm wavelength. The molar extinction coefficient for Tz-PEG$_7$-DOTA ($e_{525}$) is 535 $M^{-1}cm^{-1}$.
8. Analyze the final compound by nuclear magnetic resonance (NMR) and high-resolution mass spectrometry (HRMS) to verify that synthesis was successful. See **Table 1** for the experimentally determined chemical shifts and molecular weights of all the compounds discussed in this work.
9. Store the purified Tz-PEG$_7$-DOTA solution in the dark at -80 °C.
   NOTE: This is an acceptable stopping point in the procedure. The completed Tz-PEG$_7$-DOTA precursor is stable for at least 1 year under these conditions.

## 5. $^{177}$Lu Radiolabeling of Tz-PEG$_7$-DOTA

CAUTION: This step of the protocol involves the handling and manipulation of radioactivity. Before performing these steps — or performing any other work with radioactivity — researchers should consult with their home institution's Radiation Safety Department. Take all possible steps to minimize exposure to ionizing radiation.

NOTE: When working with small amounts of radiometals it is recommended that all buffers be free from trace metals to prevent interference in coordination site binding.

1. In a 1.7 mL centrifuge tube, add 200 µL of 0.25 M ammonium acetate buffer adjusted with aliquots of 1 M HCl to pH 5.5.
   NOTE: If using less than 370 MBq of activity for the labeling, the volume of buffer used should be reduced to 100 µL.
2. Add the desired amount of [$^{177}$Lu]LuCl$_3$ to the buffer solution. The amount added will be dependent on the number of subjects in the experiment and the radioactive doses being administered. It is recommended that 1-2 extra doses worth of radioactivity be added as a precaution to compensate for the potential loss of radioactivity during purification steps.
3. Add Tz-PEG$_7$-DOTA in DMSO to the radioactive mixture in Step 5.2. The amount of Tz-PEG$_7$-DOTA is dependent on the number of subjects being tested. More detail on this topic can be found in Step 6.2.2.2.
4. Allow the solution to incubate at 37 °C for 20 min.
5. Verify the radiolabeling is complete using radio instant thin layer chromatography (radio-iTLC) with 50 mM EDTA, pH 5.5 as the mobile phase. The labeled [$^{177}$Lu]Lu-DOTA-PEG$_7$-Tz will remain at the baseline — $R_f = 0$ — while free [$^{177}$Lu]Lu$^{3+}$ will be coordinated by the EDTA and will travel with the solvent front, $R_f = 1.0$ (**Figure 3B**).
6. If quantitative labeling is not achieved, add additional ligand to coordinate the free radiometal. Alternatively, purify the labeled [$^{177}$Lu]Lu-DOTA-PEG$_7$-Tz using a $C_{18}$ cartridge. Follow manufacturer instructions for use. A sample procedure is given below.
   1. Prime the cartridge by slowly passing through 5 mL of ethanol through the cartridge with a large syringe. Then, pass through 5 mL of acetonitrile and then 5 mL of deionized (DI) $H_2O$.
   2. Draw up the radioligand solution from Step 5.3 in a smaller syringe and inject it slowly onto the $C_{18}$ cartridge. Then, wash the cartridge with 10 mL of DI $H_2O$ to remove any unbound [$^{177}$Lu]LuCl$_3$.
   3. Elute with 500 µL of ethanol. Remove any ethanol from the final product by passing over the vessel with a low flow rate of dry nitrogen or argon for 10-15 min. Subsequently, resuspend the radioligand in saline in a volume determined in Step 6.2.2.2.

## 6. *In vivo* Studies

CAUTION: As in Section 5, this step of the protocol involves the handling and manipulation of radioactivity. Before performing these steps, researchers should consult with their home institution's Radiation Safety Department. Take all possible steps to minimize exposure to ionizing radiation.

1. **Preparation of animals**
   1. In female athymic nude mice, subcutaneously implant 5 x 10$^6$ SW1222 colorectal cancer cells suspended in 150 µL of a 1:1 mixture of cell media and matrix (*e.g.*, Matrigel) and allow these to grow into a 100-150 mm$^3$ xenograft (14-18 days after inoculation).
   2. Sorting of animals for a biodistribution experiment
      1. Once the tumors are of sufficient size as determined by caliper measurement, sort the animals to ensure each cohort has approximately the same average tumor volume. The animals can be distinguished in each cage by markings on the tail with indelible ink (one band, two bands, *etc.*).
   3. Sorting of animals for a longitudinal therapy study
      1. Once the tumors are of sufficient size as determined by caliper measurement, attach ear tags to each of the animals to ensure correct tracking throughout the experiment.
         NOTE: Numerical ear tags may fall off throughout the course of the experiment. As a result, it is recommended to accompany these physical tags with ear notches in a systematic manner (*i.e.*, right, left, bilateral, right x 2, left x 2).
      2. Sort the animals so that the average tumor volume in each cohort is roughly equal. The following method for animal sorting can be performed using a spreadsheet program.
         1. List the animal identification numbers, ear notch pattern, and tumor volume in three separate columns.
         2. Sort the data from smallest to largest tumor volume.
         3. In a fourth column, assign each animal a cage number and cycle through the cages in a snakelike pattern. For example, if there are 5 cages, this column would be filled "5, 4, 3, 2, 1, 1, 2, 3, 4, 5…" until all the animals are assigned a cage.
         4. Once the cages are assigned, sort the data by cage number. If ear notches are being used, ensure that each animal in a given cage has a unique ear notch pattern. If there are duplicates (two or more of the same pattern) in a given cage, swap one mouse with one from another cage with the missing pattern until every cage has animals with unique ear notch patterns.

2. **Formulations and Injections**
   NOTE: The sequence of injection for both biodistribution and therapy study proceeds as follows: huA33-TCO is injected first, followed by [$^{177}$Lu]Lu-DOTA-PEG$_7$-Tz after a pre-determined interval.
   1. Immunoconjugate
      1. Dilute an aliquot of the huA33-TCO solution from Step 1.9 to a concentration of 0.8 mg/mL in 0.9% sterile saline.
      2. Draw doses of 150 µL (100 µg) of huA33-TCO solution in syringes pretreated with 1% bovine serum albumin (BSA) in PBS and store these syringes on ice.
         NOTE: BSA treatment reduces the non-specific binding of the antibody to the walls of the syringe.

3. Warm the animals under a heat lamp for 3 minutes to dilate the tail vein.
4. Inject the huA33-TCO solution into the tail vein of the xenograft-bearing mouse. Allow 24 h (or a different pre-determined time interval) for the huA33-TCO to accumulate in the tumor of the mouse.

2. **Radioligand**
   1. Radiolabel Tz-$PEG_7$-DOTA as outlined in Section 5.
   2. Draw doses in 150 µL of 0.9% sterile saline containing 1.1 molar equivalents of Tz-$PEG_7$-DOTA relative to the amount of huA33-TCO administered. As an example, if 100 µg (0.67 nmol) of huA33-TCO was injected into the animal and the [$^{177}$Lu]Lu-DOTA-$PEG_7$-Tz reaction mixture was made with a specific activity of 12.4 GBq/µmol, then doses will be drawn containing 9.14 MBq of activity each. This corresponds to 0.74 nmol of Tz (1.1 molar eq. relative to huA33-TCO).
   3. Warm the animals under a heat lamp for 3 min to dilate the tail vein.
   4. Inject the dose of radioligand into the tail vein of the xenograft-bearing mouse. The amount of activity to be injected is determined by the researcher. Published data have shown dose-dependent therapeutic effects on tumor size within a range of 7.4 - 55.5 MBq.

3. **Biodistribution**
   1. At the desired time point after the administration of the radioligand, euthanize each cohort of mice using a 2% $O_2$ / 6% $CO_2$ gas mixture.
      NOTE: Follow any institutional requirements regarding methods for secondary physical euthanasia (*e.g.,* cervical dislocation).
   2. For each animal, remove all organs of interest, wash them in a water bath to remove any excess blood, and dry them on a paper towel in open air for 5 min. Sample organ list in suggested order: blood, tumor, heart, lungs, liver, spleen, stomach, small intestine, large intestine, kidneys, muscle, bone, skin, tail.
   3. Once sufficiently dried, place the organs in pre-weighed disposable culture tubes. Weigh the now-filled tubes once again to obtain the mass of each organ or tissue.
   4. Measure the activity in each of the tubes using a gamma counter. Calibrate the measured activity in the gamma counter to the detector used for measuring the drawn dose. Count radioactive standards of $^{177}$Lu on each instrument and determine a calibration factor for interconversion between activity and counts-per-minute (cpm).
   5. Plot the biodistribution data as a bar graph (see **Figure 5**) with the mean normalized uptake for each organ displayed along with a bar denoting one standard deviation. Statistical differences in uptake between sample groups may be assessed by an unpaired t-test, in which significance is achieved when $p < 0.05$.

4. **Therapy Monitoring**
   1. Using calipers, measure the longest side of the oblong tumor (length) as well as the width, which is perpendicular to the length. Calculate volume using the formula for the volume of an ellipsoid: (4/3)πL´W´H, which simplifies to ½L´$W^2$, assuming that the height is approximately equal to the width.
      NOTE: It is also possible to use a handheld tumor measuring device if one is available (see **Table of Materials**).
   2. Weigh each mouse on a balance to track weight gain or weight loss over time.
   3. Importantly, monitor each animal's physical appearance for signs of distress, such as hunched back or ruptured cutaneous blood vessels (which may indicate haematotoxicity).
      NOTE: Tumor measurements should be collected every 1-2 days during the course of the longitudinal therapy study.
   4. Plot data from the longitudinal therapy study as average tumor volumes over time and normalize to starting tumor volume if desired. Statistical differences in uptake on the same day between sample groups may be assessed by an unpaired t-test, in which significance is achieved when $P < 0.05$. More extensive statistical analyses can and should be carried out as recommended by a trained biostatistician.

## Representative Results

The conjugation of TCO to huA33 is predicated on the coupling between the amine-reactive TCO-NHS and the lysine residues on the surface of the immunoglobulin. This method is highly robust and reproducible and reliably yields a degree-of-labeling of 2-4 TCO/mAb. In this case, MALDI-ToF mass spectrometry was employed to confirm a degree of labeling of approximately 4.0 TCO/mAb; a similar value was obtained using a fluorophore-modified tetrazine as a reporter[24]. The synthesis of the tetrazine ligand is performed in three steps: (1) the coupling of Tz-NHS to a mono-Boc-protected PEG linker (2) the deprotection of this intermediate to yield Tz-$PEG_7$-$NH_2$, and (3) the formation of a thiourea linkage between *p*-SCN-Bn-DOTA and Tz-$PEG_7$-$NH_2$. This procedure is relatively facile and affords Tz-$PEG_7$-DOTA in an overall yield of ~75%. Each of the intermediates has been characterized by HRMS and $^1$H-NMR; this data is presented in **Table 1**.

Moving on to the radiolabeling, $^{177}Lu^{3+}$ is typically obtained from commercial suppliers as a chloride salt [$^{177}$Lu]$LuCl_3$ in 0.5 M HCl. The radiolabeling of Tz-$PEG_7$-DOTA with $^{177}$Lu to yield the radioligand [$^{177}$Lu]Lu-DOTA-$PEG_7$-Tz is very straightforward: in just 20 min, the reaction is complete, producing the desired product in >99% radiochemical purity as determined by radio-iTLC. Typically, no further purification is necessary prior to formulation. A survey of the literature on Tz/TCO-based pretargeting suggests that a Tz:mAb molar ratio of ~1:1 produces the best *in vivo* data[10]. As a result, it is not essential to obtain the radioligand in the highest possible molar activity. For example, biodistribution experiments discussed here employ [$^{177}$Lu]Lu-DOTA-$PEG_7$-Tz with a molar activity of ~12 GBq/µmol. For longitudinal therapy studies, in contrast, [$^{177}$Lu]Lu-DOTA-$PEG_7$-Tz with higher molar activity was used in order to facilitate the administration of larger doses of radioactivity without changing the number of injected moles of tetrazine.

As will be addressed further in the discussion, biodistribution experiments are of paramount importance to understanding and optimizing any approach to PRIT. In this case, biodistribution experiments were conducted to determine the optimal interval time between the administration of the immunoconjugate and the injection of the radioligand. To this end, we employed athymic nude mice bearing subcutaneous A33 antigen-expressing SW1222 xenografts on their right shoulder. These animals received 100 µg (0.67 nmol) of huA33-TCO 24, 48, 72, or 120 h prior to the injection of [$^{177}$Lu]Lu-DOTA-PEG$_7$-Tz (9.14 MBq, 0.74 nmol). **Figure 5** shows that all injection intervals produce high activity concentrations in the tumor tissue as well as low activity concentrations in healthy organs. The 24 h injection interval affords the highest tumoral uptake at 120 h post-injection: 21.2 ± 2.9%ID/g. Each set of conditions also produces impressive tumor-to-organ activity concentration ratios. Pretargeting with a 24 h interval, for example, yields tumor-to-blood, tumor-to-liver, and tumor-to-muscle ratios of 20 ± 5, 37 ± 7, and 184 ± 30, respectively, 120 h after the administration of the radioligand. Based on these findings, a 24 h interval was chosen for the subsequent longitudinal therapy study (see below).

For the *in vivo* longitudinal therapy study, cohorts (n = 10) of athymic nude mice bearing subcutaneous SW1222 xenografts on their right flank were administered huA33-TCO (100 ug, 0.67 nmol) 24 hours prior to injection of [$^{177}$Lu]Lu-DOTA-PEG$_7$-Tz. Three different experimental cohorts were employed, receiving 18.7, 37, or 55.5 MBq of [$^{177}$Lu]Lu-DOTA-PEG$_7$-Tz (corresponding to molar activities of 24, 45, and 70 GBq/µmol). In addition, two control cohorts received one half of the PRIT regimen: either huA33-TCO (100 ug, 0.67 nmol) without [$^{177}$Lu]Lu-DOTA-PEG$_7$-Tz *or* [$^{177}$Lu]Lu-DOTA-PEG$_7$-Tz (55.5 MBq, 0.74 nmol) without huA33-TCO. These are essential controls to ensure that the therapeutic response is not elicited by either the immunoconjugate or radioligand alone. The volumes of the tumors were measured every 3 days for the first three weeks of the study and then once per week until the conclusion of the experiment (70 days, 10 half-lives of $^{177}$Lu). As seen in **Figure 6**, there is a stark difference in the response of the experimental cohorts compared to the control groups. While the tumors in the mice receiving only one component of the PRIT strategy continue to grow unchecked, the tumors of the mice receiving the full PRIT regimen stop growing and ultimately shrink to volumes well below those measured at the beginning of the study. Importantly, no toxic side effects were observed, and all animals maintained a weight within 20% of their initial mass (**Figure 7A**). A Kaplan-Meier plot of the data provides an even more striking visualization of the study: while all mice in the control cohorts had to be euthanized within a few weeks, the mice of the experimental cohorts had a perfect record of survival at the end of the investigation (**Figure 7B**).

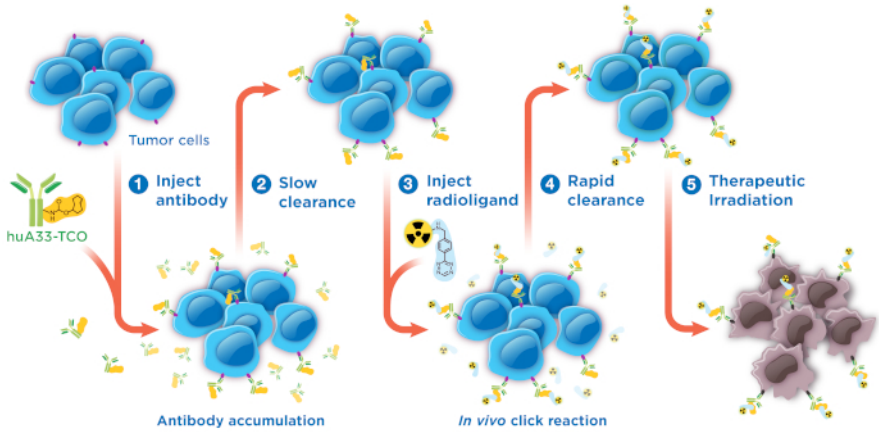


**Figure 1: Cartoon schematic of pretargeted radioimmunotherapy based on the inverse electron demand Diels-Alder reaction.** This figure has been modified from reference #28. Reprinted (adapted) with permission from Membreno, R., Cook, B. E., Fung, K., Lewis, J. S., & Zeglis, B. M. Click-Mediated Pretargeted Radioimmunotherapy of Colorectal Carcinoma. *Molecular Pharmaceutics*. **15** (4), 1729-1734 (2018). Copyright 2018 American Chemical Society. Please click here to view a larger version of this figure.

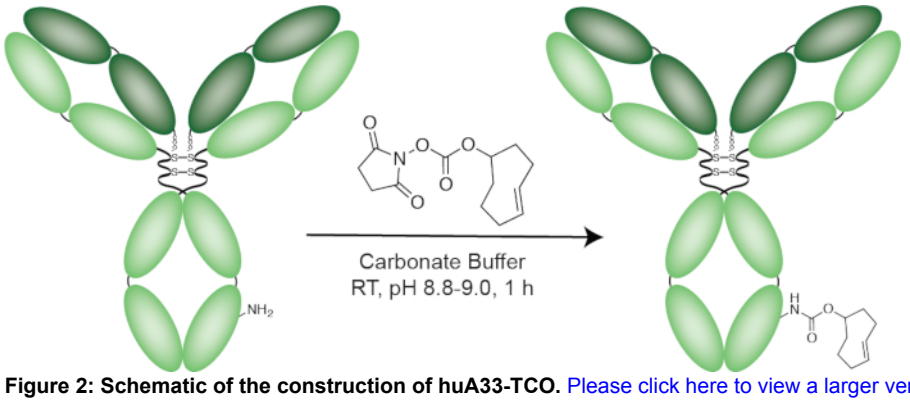


**Figure 2: Schematic of the construction of huA33-TCO.** Please click here to view a larger version of this figure.

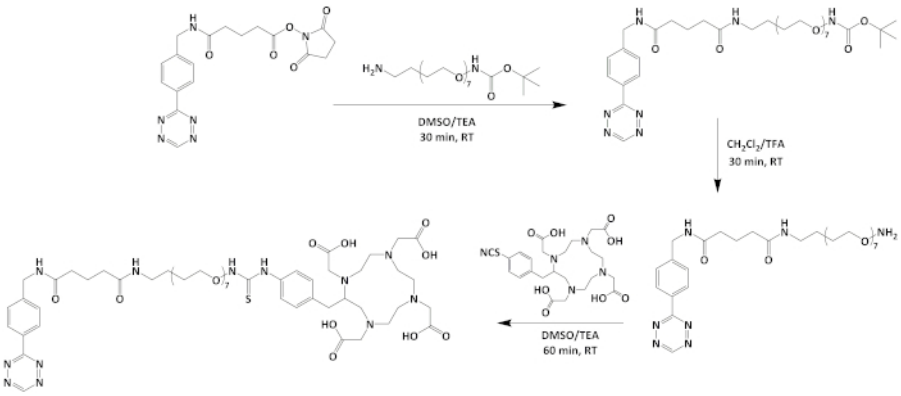


**Figure 3: Schematic of the synthesis of Tz-PEG$_7$-DOTA.** Please click here to view a larger version of this figure.

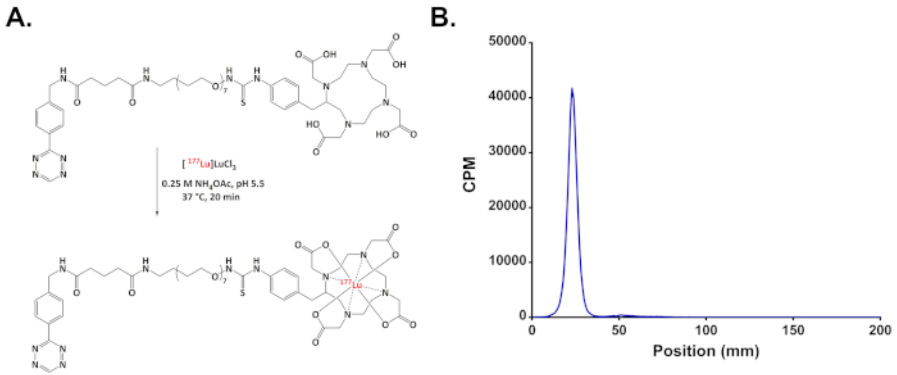


**Figure 4: (A) Schematic of the radiolabeling of [ $^{177}$Lu]Lu-DOTA-PEG$_7$-Tz; (B) Representative radio-iTLC chromatogram demonstrating the >98% radiochemical purity of [$^{177}$Lu]Lu-DOTA-PEG$_7$-Tz.** Please click here to view a larger version of this figure.

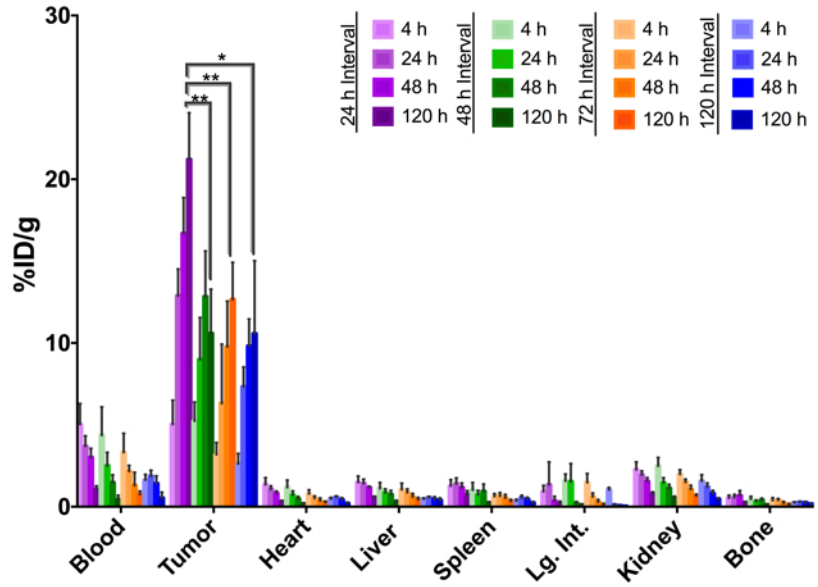


**Figure 5: Biodistribution in of *in vivo* pretargeting with huA33-TCO and [$^{177}$Lu]-DOTA-PEG$_7$-Tz in athymic nude mice bearing subcutaneous SW1222 human colorectal cancer tumors using pretargeting intervals of 24 (purple), 48 (green), 72 (orange), or 120 (blue) hours.** Data with standard errors from cohorts of n = 4; Statistical analysis was performed by an unpaired Student's t-test, $^{**}p < 0.01$. This figure has been modified from reference #28. Reprinted (adapted) with permission from Membreno, R., Cook, B. E., Fung, K., Lewis, J. S., & Zeglis, B. M. Click-Mediated Pretargeted Radioimmunotherapy of Colorectal Carcinoma. *Molecular Pharmaceutics*. **15** (4), 1729-1734 (2018). Copyright 2018 American Chemical Society. Please click here to view a larger version of this figure.

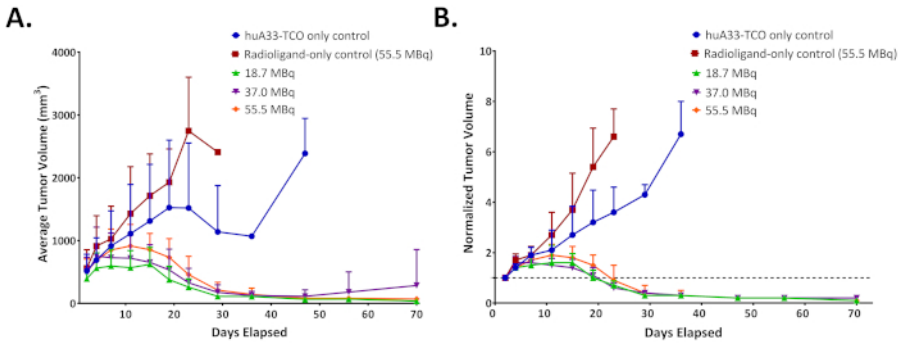


**Figure 6: Longitudinal therapy study of 5 groups of mice (n = 10 each) bearing subcutaneous SW1222 tumors depicted in average tumor volume as a function of time (A); and tumor volume normalized to initial volume as a function of time (B).** The control groups received either the immunoconjugate without the radioligand (blue) or the radioligand without the immunoconjugate (red). The three treatment groups received huA33-TCO (100 µg, 0.6 nmol) followed 24 h later by either 18.5 (green), 37.0 (purple), or 55.5 (orange) MBq (~0.8 nmol in each case) of [$^{177}$Lu]-DOTA-PEG$_7$-Tz. By log-rank (Mantel-Cox) test, survival was significant ($p < 0.0001$) for all treatment groups. This figure has been modified from reference #28. Reprinted (adapted) with permission from Membreno, R., Cook, B. E., Fung, K., Lewis, J. S., & Zeglis, B. M. Click-Mediated Pretargeted Radioimmunotherapy of Colorectal Carcinoma. Molecular Pharmaceutics. **15** (4), 1729-1734 (2018). Copyright 2018 American Chemical Society. Please click here to view a larger version of this figure.

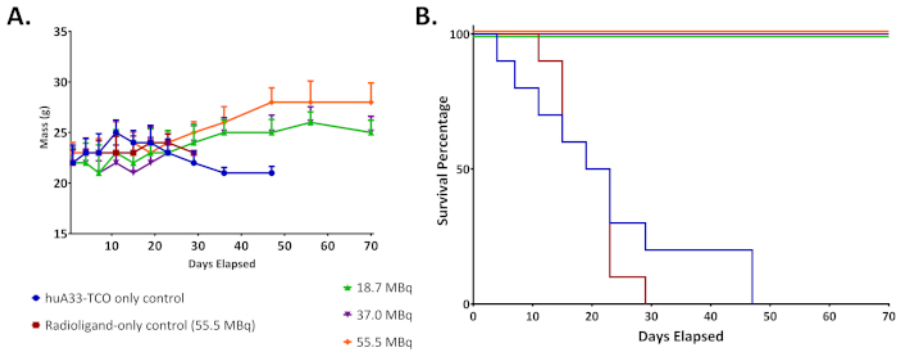


**Figure 7: Weight curves for animals during the longitudinal therapy study of 5 groups of mice (n = 10 each) bearing subcutaneous SW1222 tumors (A); the corresponding Kaplan-Meier survival curve (B).** The control groups received either the immunoconjugate without the radioligand (blue) or the radioligand without the immunoconjugate (red). The three treatment groups received huA33-TCO (100 µg, 0.6 nmol) followed 24 h later by either 18.5 (green), 37.0 (purple), or 55.5 (orange) MBq (~0.8 nmol in each case) of [$^{177}$Lu]-DOTA-PEG$_7$-Tz. This figure has been modified from reference #28. Reprinted (adapted) with permission from Membreno, R., Cook, B. E., Fung, K., Lewis, J. S., & Zeglis, B. M. Click-Mediated Pretargeted Radioimmunotherapy of Colorectal Carcinoma. *Molecular Pharmaceutics*. **15** (4), 1729-1734 (2018). Copyright 2018 American Chemical Society. Please click here to view a larger version of this figure.

| **Compound** | **$^1$H-NMR Shifts** 500 MHz, DMSO | **HRMS (ESI)** |
|---|---|---|
| Tz-PEG$_7$-NHBoc | 10.52 (s, 1H), 8.50 (m, 3H), 7.82 (t, 1H), 7.46 (d, 2H), 6.69 (t, 1H), 4.33 (d, 2H), 3.42 (m, 22H), 3.33 (t, 2H), 3.31 (t, 2H), 3.12 (q, 2H), 2.99 (q, 2H), 2.12 (t, 2H), 2.03 (t, 2H), 2.12 (t, 2H), 1.70 (q, 2H), 1.29 (s, 9H) | *m/z* calcd. for $C_{35}H_{57}N_7O_{11}Na$: 774.4005; found: 774.4014. |
| Tz-PEG$_7$-NH$_2$ | 10.58 (s, 1H), 8.46 (m, 2H), 7.87 (t, 1H), 7.75 (d, 2H), 7.52 (d, 1H), 4.40 (d, 2H), 3.60-3.50 (m, 26H), 3.40 (t, 2H), 3.32 (bs, 2H), 3.20 (q, 2H), 2.99 (bs, 2H), 2.19 (t, 2H), 2.12 (t, 2H), 1.79 (q, 2H). | *m/z* calcd. for $C_{30}H_{50}N_7O_9$: 652.3670; found: 652.3676. |
| Tz-PEG$_7$-DOTA | 10.57 (s, 1H), 9.63 (bs, 1H), 8.45 (m, 3H), 7.86 (m, 1H), 7.73 (bs, 1H), 7.54 (d, 2H), 7.41 (m, 2H), 7.19 (m, 2H), 6.54 (bs, 1H), 4.40 (d, 2H), 4.00-3.20 (m, 55H), 3.20 (q, 4H), 2.54 (s, 1H), 2.18 (t, 3H), 2.10 (t, 3H), 1.76 (q, 2H). | *m/z* calcd. for $C_{50}H_{76}N_{11}O_{15}S$: 1202.56; found: 1203.5741. |

**Table 1.** Characterization data for the organic compounds described in this protocol.

## Discussion

One of the strengths of this approach to *in vivo* pretargeting — especially in relation to strategies predicated on bispecific antibodies and radiolabeled haptens — is its modularity: *trans*-cyclooctene moieties can be appended to any antibody, and tetrazine radioligands can be radiolabeled with an extraordinary variety of radionuclides without impairing their ability to react with their click partners. Yet the adaptation of this approach to other antibody/antigen system is not as simple as duplicating the protocol described here. Of course, any attempt to create a new mAb-TCO immunoconjugate or a novel tetrazine-bearing radioligand should be accompanied by the appropriate chemical and biological characterization assays, including tests for stability and reactivity. But beyond this, there are two variables that are particularly important to explore and optimize: (1) the mass of mAb-TCO immunoconjugate administered and (2) the interval time between the injection of the mAb-TCO and the administration of the radioligand. Both factors can dramatically influence the *in vivo* behavior of the pretargeting system. For example, the use of overly high doses of immunoconjugate or interval periods that are too short can result in undesirably high activity concentrations in the blood due to click reactions between the radioligand and immunoconjugate remaining in circulation. Conversely, employing masses of immunoconjugate that are too low or overly long interval periods can needlessly reduce activity concentrations in the tumor due to a failure to saturate the antigen or the inexorable (though slow) isomerization of the *trans*-cyclooctene to inactive *cis*-cyclooctene. Along these lines, performing biodistribution experiments using a range of masses of immunoconjugate and pretargeting intervals can be extraordinarily helpful. Of course, it is also recommended that appropriate controls be run in tandem with any *in vivo* experiments. These include — but are not limited to — experiments featuring antigen-negative cell lines, blocking cohorts that receive a vast excess of unconjugated antibody, the administration of the radioligand alone, the injection of the radioligand following a TCO-*lacking* immunoconjugate, and *in vivo* pretargeting using a non-specific, isotype control TCO-bearing immunoconjugate.

Alternatively, imaging experiments can be used for optimization if the therapeutic radionuclide emits positrons or 'imageable' photons *or* if an 'imageable' isotopologue of the therapeutic radionuclide is available. Ultimately, the sets of variables that provide the best balance of high tumoral activity concentrations and high tumor-to-background activity concentration ratios should be selected for subsequent longitudinal therapy studies. In the case presented here, 100 µg of huA33-TCO was injected with an interval of 24 h. Dosimetry calculations — particularly those that allow for the calculation of tumor doses and therapeutic ratios — can also be helpful during the process of optimization.

It is important to note that even the promising [$^{177}$Lu]Lu-DOTA-PEG$_7$-Tz/huA33-TCO system that has been developed could benefit from additional optimization. A comparison between the dosimetry data from this approach to PRIT and traditional RIT with a $^{177}$Lu-labeled variant of huA33 reveals that the tumor dose of PRIT lies below that of traditional RIT. Furthermore, the effective dose of the PRIT system (0.054 mSv/MBq) is only slightly lower than that of traditional RIT (0.068 mSv/MBq).

Two remedies to these issues are currently being explored. First, a dendritic scaffold has been developed capable of increasing the number of TCOs appended to each antibody[30]. In the context of pretargeted PET imaging, this approach dramatically boosts tumoral activity concentrations, and analogous experiments with [$^{177}$Lu]Lu-DOTA-PEG$_7$-Tz are underway. Second, the use of tetrazine-bearing clearing agents may be useful in the context of PRIT. The administration of clearing agents prior to the injection of the radioligand has been exploited in a variety of pretargeting methodologies as a way to decrease the concentration of residual immunoconjugate in the blood and thus reduce activity concentrations in healthy organs[23,31]. The use of clearing agents is not without its drawbacks, though; the most notable of which is increasing the complexity of an already admittedly complicated therapeutic modality. Nonetheless, researchers at Memorial Sloan Kettering Cancer Center recently published a compelling report on the creation a Tz-labeled dextran clearing agent for pretargeted PET imaging, and data on the use of this construct in conjunction with [$^{177}$Lu]Lu-DOTA-PEG$_7$-Tz and huA33-TCO are forthcoming[32]. Another approach to maximizing the dosimetric benefits of PRIT is the use of radionuclides with shorter physical half-lives. This has proven highly effective for imaging; however, therapeutic radionuclides with short physical half-lives are few and far between.

Finally, we would be remiss if we failed to properly address some of the intrinsic limitations of pretargeting based on the inverse electron demand Diels-Alder reaction. The first of these problems is inherent to *all* approaches to *in vivo* pretargeting: the antibody employed cannot be internalized upon binding to the target tissue. This, of course, is essential, as the antibody must remain accessible to the radioligand rather than sequestered in an intracellular compartment. This limitation is admittedly hard to circumvent, though it has been shown recently that antibodies with slow-to-moderate rates of internalizing *can* be used for *in vivo* pretargeting[33,34]. Second, the slow *in vivo* isomerization of reactive *trans*-cyclooctene to inactive *cis*-cyclooctene has the potential to limit the length of the interval between the administration of the TCO-bearing immunoconjugate and the injection of the radioligand. Critically, intervals of up to 120 h have still provided excellent results in the context of both pretargeted PET imaging *and* PRIT. However, the use of these longer intervals is almost always accompanied by slight reductions in tumoral activity concentrations, a result which may stem from this isomerization. In order to address this issue, several laboratories have attempted to create more stable *trans*-cyclooctenes without compromising reactivity, while others have tried to develop entirely new dienophiles capable of reacting with tetrazine[35]. In the coming years, it is our hope that these chemical developments will be leveraged for PRIT.

In the end, PRIT based on the inverse electron demand Diels-Alder ligation is undeniably an emergent and somewhat immature technology. However, we are nonetheless encouraged by the preclinical results we have obtained and excited for the clinical promise of this strategy. We sincerely hope that this protocol encourages others to explore and optimize this approach and thus fuel its journey from the laboratory to the clinic.

## Disclosures

The authors have nothing to disclose.

## Acknowledgements

The authors thank Dr. Jacob Houghton for helpful conversations.

## References

1. Goldenberg, D. M. Targeted Therapy of Cancer with Radiolabeled Antibodies. *Journal of Nuclear Medicine.* **43** (5), 693-713 (2002).
2. Goldenberg, D. M. *et al.* Targeting, Dosimetry, and Radioimmunotherapy of B-cell Lymphomas with Iodine-131-labeled LL2 Monoclonal Antibody. *Journal of Clinical Oncology.* **9** (4), 548-564 (1991).
3. Kaminski, M. S. *et al.* Radioimmunotherapy with 131I-Tositumomab for Relapsed or Refractory B-cell non-Hodgkin Lymphoma: Updated Results and Long-Term Follow-Up of the University of Michigan Experience. *Blood.* **96** (4), 1259-1266 (2000).
4. Davies, A. J. Radioimmunotherapy for B-cell Lymphoma: Y90 Ibritumomab Tiuxetan and I131 Tositumomab. *Oncogene.* **26** 3614 (2007).
5. Rajendran, J. *et al.* Comparison of Radiation Dose Estimation for Myeloablative Radioimmunotherapy for Relapsed or Recurrent Mantle Cell Lymphoma Using 131I Tositumomab to That of Other Types of Non-Hodgkin's Lymphoma. *Cancer Biotherapy and Radiopharmaceuticals.* **19** (6), 738-745 (2004).
6. Rajendran, J. G. *et al.* High-Dose 131I-Tositumomab (Anti-CD20) Radioimmunotherapy for Non-Hodgkin's Lymphoma: Adjusting Radiation Absorbed Dose to Actual Organ Volumes. *Journal of Nuclear Medicine.* **45** (6), 1059-1064 (2004).
7. Larson, S. M., Carrasquillo, J. A., Cheung, N.-K. V., & Press, O. Radioimmunotherapy of Human tumours. *Nature Reviews Cancer.* **15** (6), 347-360 (2015).
8. Kelly, M. P. *et al.* Tumor Targeting by a Multivalent Single-Chain Fv (scFv) Anti-Lewis Y Antibody Construct. *Cancer Biotherapy & Radiopharmaceuticals.* **23** (4), 411-423 (2008).
9. Yazaki, P. J. *et al.* Tumor Targeting of Radiometal Labeled Anti-CEA Recombinant T84.66 Diabody and T84.66 Minibody: Comparison to Radioiodinated Fragments. *Bioconjugate Chemistry.* **12** (2), 220-228 (2001).
10. van Duijnhoven, S. M. J. *et al.* Diabody Pretargeting with Click Chemistry In Vivo. *Journal of Nuclear Medicine.* **56** (9), 1422-1428 (2015).
11. Altai, M., Membreno, R., Cook, B., Tolmachev, V., & Zeglis, B. M. Pretargeted Imaging and Therapy. *Journal of Nuclear Medicine.* **58** (10), 1553-1559 (2017).
12. Goldenberg, D. M., Chatal, J.-F., Barbet, J., Boerman, O., & Sharkey, R. M. Cancer Imaging and Therapy with Bispecific Antibody Pretargeting. *Update on cancer therapeutics.* **2** (1), 19-31 (2007).
13. Rossin, R. *et al.* In Vivo Chemistry for Pretargeted Tumor Imaging in Live Mice. *Angewandte Chemie International Edition.* **49** (19), 3375-3378 (2010).
14. Gestin, J. F. *et al.* Two-Step Targeting of Xenografted Colon Carcinoma Using a Bispecific Antibody and 188Re-Labeled Bivalent Hapten: Biodistribution and Dosimetry Studies. *Journal of Nuclear Medicine.* **42** (1), 146-153 (2001).
15. Green, D. J. *et al.* Comparative Analysis of Bispecific Antibody and Streptavidin-Targeted Radioimmunotherapy for B-cell Cancers. *Cancer Research.* **76** (22), 6669 (2016).
16. Sharkey, R. M. *et al.* Development of a Streptavidin−Anti-Carcinoembryonic Antigen Antibody, Radiolabeled Biotin Pretargeting Method for Radioimmunotherapy of Colorectal Cancer. Studies in a Human Colon Cancer Xenograft Model. *Bioconjugate Chemistry.* **8** (4), 595-604 (1997).
17. Knox, S. J. *et al.* Phase II Trial of Yttrium-90-DOTA-Biotin Pretargeted by NR-LU-10 Antibody/Streptavidin in Patients with Metastatic Colon Cancer. *Clinical Cancer Research.* **6** (2), 406 (2000).
18. Schubert, M. *et al.* Novel Tumor Pretargeting System Based on Complementary L-Configured Oligonucleotides. *Bioconjugate Chemistry.* **28** (4), 1176-1188 (2017).
19. Forero, A. *et al.* Phase 1 Trial of a Novel Anti-CD20 Fusion Protein in Pretargeted Radioimmunotherapy for B-cell Non-Hodgkin Lymphoma. *Blood.* **104** (1), 227 (2004).
20. Kalofonos, H. P. *et al.* Imaging of Tumor in Patients with Indium-111-Labeled Biotin and Streptavidin-Conjugated Antibodies: Preliminary Communication. *Journal of Nuclear Medicine.* **31** (11), 1791-1796 (1990).
21. Zeglis, B. M. *et al.* A Pretargeted PET Imaging Strategy Based on Bioorthogonal Diels-Alder Click Chemistry. *Journal of Nuclear Medicine.* **54** (8), 1389-1396 (2013).
22. Meyer, J.-P. *et al.* 18F-Based Pretargeted PET Imaging Based on Bioorthogonal Diels-Alder Click Chemistry. *Bioconjugate Chemistry.* **27** (2), 298-301 (2016).
23. Rossin, R., Läppchen, T., van den Bosch, S. M., Laforest, R., & Robillard, M. S. Diels-Alder Reaction for Tumor Pretargeting: In Vivo Chemistry Can Boost Tumor Radiation Dose Compared with Directly Labeled Antibody. *Journal of Nuclear Medicine.* **54** (11), 1989-1995 (2013).
24. Zeglis, B. M. *et al.* Optimization of a Pretargeted Strategy for the PET Imaging of Colorectal Carcinoma *via* the Modulation of Radioligand Pharmacokinetics. *Molecular Pharmaceutics.* **12** (10), 3575-3587 (2015).
25. Agard, N. J., Prescher, J. A., & Bertozzi, C. R. A Strain-Promoted [3 + 2] Azide−Alkyne Cycloaddition for Covalent Modification of Biomolecules in Living Systems. *Journal of the American Chemical Society.* **126** (46), 15046-15047 (2004).
26. Blackman, M. L., Royzen, M., & Fox, J. M. Tetrazine Ligation: Fast Bioconjugation Based on Inverse-Electron-Demand Diels−Alder Reactivity. *Journal of the American Chemical Society.* **130** (41), 13518-13519 (2008).
27. Houghton, J. L. *et al.* Establishment of the In Vivo Efficacy of Pretargeted Radioimmunotherapy Utilizing Inverse Electron Demand Diels-Alder Click Chemistry. *Molecular Cancer Therapeutics.* **16** (1), 124-133 (2017).
28. Membreno, R., Cook, B. E., Fung, K., Lewis, J. S., & Zeglis, B. M. Click-Mediated Pretargeted Radioimmunotherapy of Colorectal Carcinoma. *Molecular Pharmaceutics.* **15** (4), 1729-1734 (2018).
29. Reiner, T., Lewis, J. S., & Zeglis, B. M. Harnessing the Bioorthogonal Inverse Electron Demand Diels-Alder Cycloaddition for Pretargeted PET Imaging. *Journal of Visualized Experiments.* (96), e52335 (2015).
30. Cook, B. E., Membreno, R., & Zeglis, B. M. Dendrimer Scaffold for the Amplification of In Vivo Pretargeting Ligations. *Bioconjugate Chemistry.* **29** (8), 2734-2740 (2018).

 

31. Cheal, S. M. *et al.* Theranostic Pretargeted Radioimmunotherapy of Colorectal Cancer Xenografts in Mice Using Picomolar Affinity Y-86- or Lu-177-DOTA-Bn Binding scFv C825/GPA33 IgG Bispecific Immunoconjugates. *European journal of nuclear medicine and molecular imaging.* **43** (5), 925-937 (2016).
32. Meyer, J.-P. *et al.* Bioorthogonal Masking of Circulating Antibody-TCO Groups Using Tetrazine-Functionalized Dextran Polymers. *Bioconjugate Chemistry.* **29** (2), 538-545 (2018).
33. Houghton, J. L. *et al.* Pretargeted Immuno-PET of Pancreatic Cancer: Overcoming Circulating Antigen and Internalized Antibody to Reduce Radiation Doses. *Journal of Nuclear Medicine.* **57** (3), 453-459 (2016).
34. Keinänen, O. *et al.* Pretargeting of Internalizing Trastuzumab and Cetuximab with a (18)F-Tetrazine Tracer in Xenograft Models. *European Journal of Nuclear Medicine and Molecular Imaging Research.* **7,** 95 (2017).
35. Billaud, E. M. F. *et al.* Micro-flow Photosynthesis of New Dienophiles for Inverse-Electron-Demand Diels-Alder Reactions. Potential Applications for Pretargeted In Vivo PET Imaging. *Chemical Science.* **8** (2), 1251-1258 (2017).


 